



SURFACE EXCHANGES IN A MESOSCALE
MODEL OF THE ATMOSPHERE.

K M CARPENTER

NOTE: This paper has not been published. Permission to quote from it must be obtained from the Assistant Director of the above Meteorological Office Branch.

Surface Exchanges in a Mesoscale Model of the Atmosphere.

K M Carpenter,
Meteorological Office
Bracknell

Introduction

In this talk I shall describe:

1. the Met Office mesoscale model
2. the description of surface exchanges in the mesoscale model.
3. a simple experiment to discover, in selected situations, the comparative effects of varying the parameters that determine the nature of the surface.
4. the effect of varying the surface resistance to evaporation on a simulated sea breeze in Florida.

The Mesoscale Model

The basic formulation of the model has been described by Tapp and White (1976). It was developed as a prototype local weather forecast model, and also in order to study the whole range of mesoscale phenomena e.g. rainbands on fronts, gales, sea breezes and convective storms. The study of mesoscale systems is carried out because it is interesting, because an understanding of the controlling mechanisms will hopefully lead to improved forecasts and in order to improve the parameterisation of mesoscale phenomena in larger scale models.

There are two aspects to modelling local weather systems. The effects of orography and topography require a full three dimensional model of the sort developed by Tapp and White, but many features of boundary layer structure (e.g. the clearing of stratocumulus) can probably be modelled very well with a one-dimensional model. These two aspects come together in the study of sea breezes, for which the effects of orography and topography are of basic importance but for which the timing, vigour and inland penetrative could be sensitive to the surface exchanges of heat and momentum. An example showing 50 m wind forecast by the mesoscale model for the

U.K. on a good sea breeze day is given in Fig 1.

In the form that produced the forecast shown in Fig 1, the model has a grid of 61 x 61 points and 10 levels. The horizontal grid length is 10 km, and the levels are at irregular intervals with the lowest level at 50m and the highest at 4000m. The finite difference scheme is (mostly) second order accurate and uses a staggered grid. The model equations are

$$\frac{Du}{Dt} - f v = -c_p \theta \frac{\partial P}{\partial x} + \kappa \nabla_H^2 u + \frac{\partial}{\partial z} k_M \frac{\partial u}{\partial z} \quad (1)$$

$$\frac{Dv}{Dt} + f u = -c_p \theta \frac{\partial P}{\partial y} + \kappa \nabla_H^2 v + \frac{\partial}{\partial z} k_M \frac{\partial v}{\partial z} \quad (2)$$

$$\frac{Dw}{Dt} = -g - c_p \theta \frac{\partial P}{\partial z} + \kappa \nabla_H^2 w \quad (3)$$

$$\frac{D\theta}{Dt} = \kappa \nabla_H^2 \theta + \frac{\partial}{\partial z} k_H \frac{\partial \theta}{\partial z} \quad (4)$$

$$\frac{DP}{Dt} = -(\gamma-1) \nabla \cdot \underline{v} + (\gamma-1) \frac{P}{\theta} \frac{D\theta}{Dt} \quad (5)$$

where θ is potential temperature

and the pressure variable P is the Exner function

$$P = \left(\frac{P}{P_r} \right)^{R/c_p}$$

The remaining rotation is standard.

Boundary layer turbulence is modelled through the vertical diffusion term on the right of equations 1 to 4. By implication, the flux of any quantity is always down the gradient. There remains the problem of specifying the diffusion coefficients. The present calculation of these coefficients has only a weak basis in theory or observation, but is designed to ensure the development of a well mixed boundary layer capped by a sharp

inversion in dry conditions with strong surface heating. The diffusion coefficient close to the surface ensures continuity with the surface fluxes, and the diffusion coefficient at the level of the inversion ensures a downward heat flux which is a fixed fraction (0.2) of the upward heat flux at the surface. Carson(1973), Tennekes(1973).

There is a convective adjustment in the model that prevents lapse rate instability developing. The hydrological cycle and orography have been included in other versions of the model, but are absent from the model giving the results shown here. Similarly, the effects of radiation are excluded except insofar as they (and humidity) are required in order to calculate the surface exchanges.

Surface Exchanges

If

$\underline{\tau}$ is the surface flux of momentum (a vector)

H is the surface flux of sensible heat

E is the surface flux of water vapour

G is the heat flux into the ground and

R is the net radiation flux into the surface

$$R = H + LE + G \quad (6)$$

$$H = \rho_a c_p c_H |u| (\theta_0 - \theta_1) \quad (7)$$

$$E = \rho_a c_H |u| (q_0 - q_1) \quad (8)$$

$$\underline{\tau} = \rho_a c_D |u| \underline{u} \quad (9)$$

where ρ_a is the density of air,

c_D and c_H are both transfer coefficients and

q is humidity mixing ratio.

Suffix "0" indicates a surface value, and suffix "1" a value at the lowest model level.

Over the sea the surface temperature and humidity are held constant (100% relative humidity) and the roughness length z_0 used in the calculation of C_D and C_H (see below) is always 10^{-4} m.

The net radiation is given by

$$R = S + B_1 - B_0 \quad (10)$$

where S is the specified solar radiation (after taking account of albedo and atmospheric absorption),

$$B_0 = \sigma \theta_0^4$$

is the long wave cooling of the surface and

$$B_1 = a \sigma \theta_1^4 \quad (a = 0.68)$$

is the downward flux of long wave radiation, which has been calculated from the temperature at the lowest model level⁽¹⁾.

The heat flux into the ground is calculated using a two level model that is intended to reproduce the properties of uniform homogenous soil. The equations governing the diffusion of heat in such an ideal medium are

$$\frac{\partial \theta(z, t)}{\partial t} = K \frac{\partial^2 \theta(z, t)}{\partial z^2} \quad (11)$$

$$K \left. \frac{\partial \theta}{\partial z} \right|_{z=0} = \frac{G}{\rho_s c_s} \quad (12)$$

where z is depth into the ground,

ρ_s is soil density

c_s is soil specific heat capacity and

K is soil thermal diffusivity.

By replacing the depth z by

$$z' = z / \sqrt{K}$$

all parameters except $\rho_s c_s \sqrt{\pi}$ can be eliminated from 11 and 12. The model used for G is

$$G = \rho_s c_s \sqrt{\pi} \left(\frac{1}{h_1} \frac{\partial \theta_0}{\partial t} + F \right) \quad (13)$$

$$F = \frac{1}{h_2} \frac{\partial \theta_s}{\partial t} = \lambda (\theta_0 - \theta_s) \quad (14)$$

where $h_1 (= 43.58 \text{ S.I.})$, $h_2 (= 212 \text{ S.I.})$ and $\lambda (= 8.54 \times 10^{-3} \text{ S.I.})$ are chosen so that equations 13 and 14 reproduce the properties of 11 and 12 for variations with periods of a day or less, and θ_s is a "soil temperature".

A comparison between ground heat fluxes calculated from 13 and 14 and from 11 and 12 is given in Fig 2. Fig 3 shows that the ground heat flux can have a maximum comparable with those of the other heat fluxes⁽²⁾ if the value chosen for $\rho_s c_s \sqrt{\pi}$ is typical of slightly moist soil (950 mks).

In addition equation 8, the surface evaporation is given by

$$E = \rho_a \frac{q_{\text{sat}}(\theta_0) - q_0}{r} \quad (15)$$

which incorporates the idea of a surface resistance to evaporation (Monteith(1964)). The surface mixing ratio q_0 can be eliminated from 8 and 15, and is never calculated in the present model.

$$E = \rho_a c_H |u| \frac{1}{1 + r c_H |u|} (q_{\text{sat}}(\theta_0) - q_1) \quad (16)$$

The humidity difference

$$q_0 - q_1 = \frac{q_{\text{sat}}(\theta_0) - q_1}{1 + r c_H |u|} \quad (17)$$

is required for the calculation of the surface layer stability parameter R_i (equation 19). The surface resistance r is calculated by specifying a value r_s that is believed to be typical during the day of the vegetation, soil conditions and season appropriate to the current study, and then using

* In both cases the full surface exchanges scheme described in the text was used with specified incident solar radiation.

$$\Gamma = 0 \quad \text{if} \quad E < 0 \quad (\text{dew forming})$$

$$\Gamma = \Gamma_s \quad \text{if} \quad E > 0, S > 0 \quad (\text{day})$$

$$\Gamma = 3\Gamma_s \quad \text{if} \quad E > 0, S = 0 \quad (\text{night})$$

This diurnal variation of Γ 's is believed to be broadly realistic, but ignores the effects of increasing physiological stress during the day, and can have the interesting effect illustrated in Fig 4 at dawn and dusk.

The equations for the surface fluxes are closed by the specification of the bulk transfer coefficients C_D and C_H . These are functions of two dimensionless numbers, which are

z/z_0 , where z is the height of the lowest level and z_0 is the roughness length, and the bulk Richardson number Ri ,

$$Ri = \frac{g z}{\theta_1 u^2} (\theta_1 - \theta_0 + 0.61 \theta_1 (q_1 - q_0)) \quad (19)$$

and are calculated by bi-linear interpolation between entries in a table. The table of values for C_D and C_H has been calculated from Monin - Obukhov similarity theory, which gives

$$C_H = \frac{\kappa^2}{\int_{\xi_0}^{\beta} \phi_H(\xi) \frac{d\xi}{\xi} \int_{\xi_0}^{\beta} \phi_H(\xi) \frac{d\xi}{\xi}} \quad (20)$$

$$C_D = \frac{\kappa^2}{\left[\int_{\xi_0}^{\beta} \phi_M(\xi) \frac{d\xi}{\xi} \right]^2} \quad (21)$$

where $\beta = z/L$, $\xi_0 = z_0/L$

L is the Monin - Obukhov length

$$L = \left| \frac{C_D^{3/2}}{\kappa C_H Ri} \right| z \quad (22)$$

κ is the von-Karmon constant (0.4 is used) and

ϕ_H and ϕ_M are the Monin - Obukhov similarity functions defined by

$$\frac{\partial \theta}{\partial z} = \frac{\theta_*}{\kappa z} \phi_H \left(\frac{z}{L} \right) \quad (23)$$

$$\frac{\partial u}{\partial z} = \frac{u_*}{\kappa z} \phi_M \left(\frac{z}{L} \right) \quad (24)$$

in the usual notation. The expressions used for ϕ_H and ϕ_M are

$$\begin{aligned} \phi &= (1 + 5 \frac{z}{L}) & \text{for } z \leq 1 \\ &= 6 & \text{for } z > 1 \end{aligned} \quad (25)$$

in stable conditions (Webb(1970))

$$\phi_M = (1 + 15 \frac{z}{L})^{-0.275} \quad (26)$$

$$\phi_H = (1 + 15 \frac{z}{L})^{-0.55} \quad (27)$$

in unstable conditions (Dyer(1971)).

In very unstable conditions this calculation is abandoned in favour of free convection similarity theory, which gives

$$c_H \propto \int \left\{ \frac{R_i}{(\exp^{z/z_0} - 1)^3} \right\} \quad (28)$$

The transition between the two expressions is made, for given z/z_0 , at the value of R_i for which they give equal $\frac{\partial c_H}{\partial R_i}$. The constant of proportionality in equation 28 is fixed by imposing continuity at the transition.

Varying the Surface Parameters

In the model described above there are only three parameters available to describe the nature of the surface.

$\rho_s c_s \sqrt{\kappa}$	(ground heat flux)
z_0	(roughness length)
r_s	(surface resistance to evaporation)

In order to assess the comparative and absolute effect of using different values for these parameters, the surface exchanges model was integrated with different values for the parameters for three days (the third day gives the same results as the second day) with the atmospheric conditions at $z = 10\text{m}$ held constant.

Five sets of values for the surface parameters* were used

1	$z_0 = 5 \text{ cm},$	$e c \sqrt{K} = 400 \text{ mks},$	$r_s = 50 \text{ sec m}^{-1}$
2	20 cm	400	50
3	5	1400	50
4	5	400	100
5	5	400	50

and 5 sets of atmospheric conditions at 10 metres were used (25 integrations in all)

A	$\theta_1 = 280$	$q_v = 0.01$	$ u = 5 \text{ m sec}^{-1}$
B	290	0.015	2 m sec^{-1}
C	285	0.01	2 m sec^{-1}
D	290	0.015	5 m sec^{-1}
E	285	0.01	5 m sec^{-1}

The solar radiation represented a clear spring day in England.

The surface parameters are the same for 1 and 5, but the definition of the bulk Richardson number R_i was modified in 5 in order to assess the importance of a correct calculation of the transfer coefficients C_D and C_H ; the calculation used in 5 was

$$R_i = \frac{g z}{\theta u^2} (\theta_1 - \theta_0 + \lambda)$$

The results from B and C were similar, as were those from D and E.

* A realistic range of z_0 values is rather higher than values that are usually observed because hedges, buildings and trees will introduce effects that are usually deliberately ignored. $e c \sqrt{K} = 400$ is a reasonable value for a wide range of dry soils, $e c \sqrt{K} = 1400$ is reasonable for a wide range of moist soils. $r_s = 50 \text{ sec m}^{-1}$ is slightly high for grassland $r_s = 100 \text{ sec m}^{-1}$ is typical for forests.

Fig 5 gives the surface exchanges in case A1, and Fig 6 shows the sensible heat flux for the 5 different surfaces. In this situation changing z_0 had the most effect, varying r_s had a comparable effect but no change was very significant.

Fig 7 shows the sensible heat fluxes for situations B. In this case changing the surface resistance r_s has the most marked effect, and changing $e c \sqrt{u}$ has some effect. Figs 8 and 9 show the surface fluxes for case B with, respectively, low and high values for r_s (surfaces 1 and 4).

Fig 10 shows the surface fluxes for situation D, and Fig 11 the comparative sensible heat fluxes for case D. Here again, changing r_s has the most effect during the day, but at night the sensible heat flux is sensitive to the calculation of the transfer coefficients C_D and C_H . This is probably because the sensible heat flux is not a monotonic function (for given wind speed) of the surface temperature in stable conditions, a fact that should be expected to cause problems in a 3D modelling context.

These comparisons, in particular that between Figs 8 and 9, show the importance of the surface resistance to the calculation of the surface exchanges, in particular the sensible heat flux.

Florida Sea Breeze Case Study

The remaining figures show the effect on a simulation of sea breezes over Florida of varying the surface resistance to evaporation. The values used for were $50 \text{ sec metre}^{-1}$ and $100 \text{ sec metre}^{-1}$ and it is quite clear that the higher surface resistance produces a more intense sea breeze that penetrates some 20 km further inland.

Conclusions

It seems that the surface resistance to evaporation is the most important surface parameter in determining the calculation of surface exchanges. The surface resistance is well known to depend on the crop covering the surface, the condition

of the crop and the condition and nature of the soil. In the present context, the values chosen should not represent a single crop but a variable combination of roads, hedges, rivers and forests all of which can be present in a 10 km square.

Footnote

(1) Mr J B Stewart suggested that 0.68 were a rather low value for α . I replied that the present value gave a low equilibrium value for surface temperature at night and this experience suggested that he was correct.

(2) Prof J L Monteith pointed out that ground heat fluxes of this magnitude are not observed beneath vegetation cover, and suggested that this may be because of the insulating layer of air trapped by the vegetation. I agreed, but pointed out the difficulty of describing the variation between deep vegetation cover and no vegetation that could occur within an area of 100 km².

References

- Carson, D.J. (1973) "The development of a dry inversion capped convectively unstable boundary layer"
Q.J.Roy.Met.Soc. 99
- Monteith, J.L. (1964) "Evaporation and environment"
Signip.Soc.Exp.Bio. 19
- Tapp M,C and (1976) "A non-hydrostatic mesoscale model"
White P.W. Q.J.Roy.Met.Soc. 102
- Tennekes H (1973) "A model of the dynamics of the inversion above a convective boundary layer".
Journ.Atmos.Sci. 30

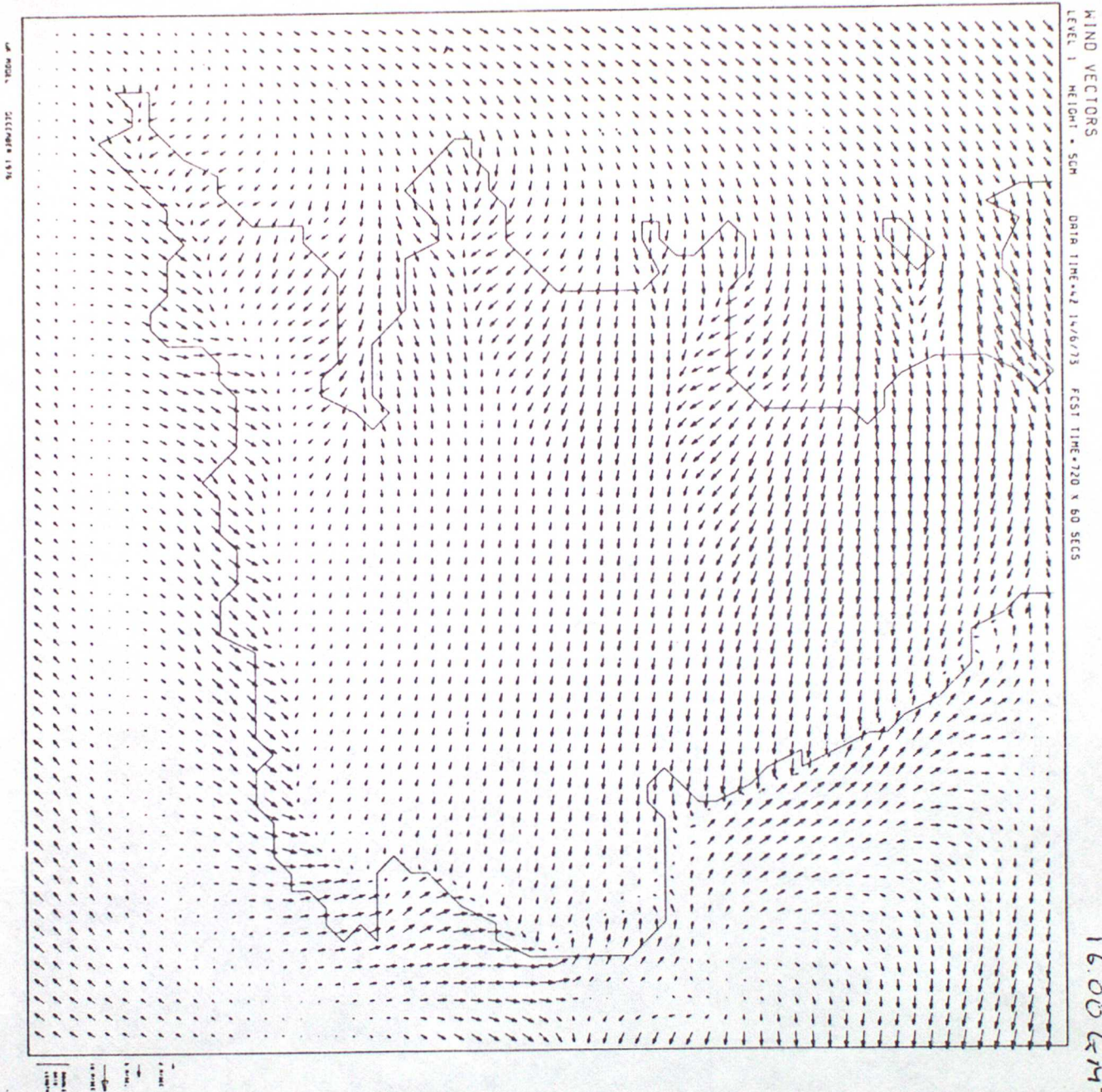


Fig 1 50m winds forecast by the mesoscale model on a good sea breeze day (14 June 1973).

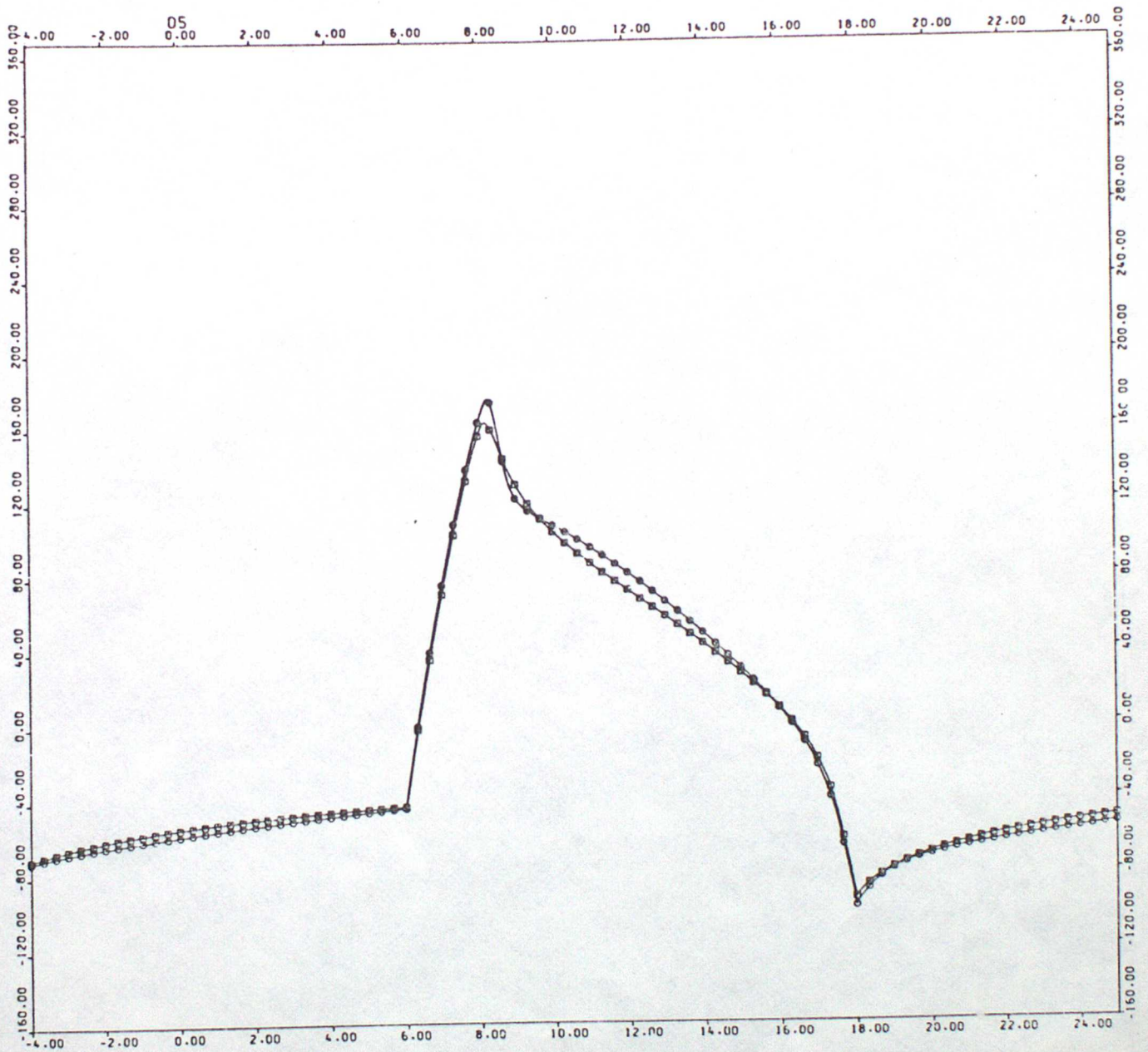


Fig 2 Comparison between the ground heat fluxes calculated from the full equations for heat diffusion in ideal soil and from the simple two level model described in the text.

- NET RADIATION
- SENSIBLE HEAT FLUX
- △ LATENT HEAT FLUX
- + GROUND HEAT FLUX

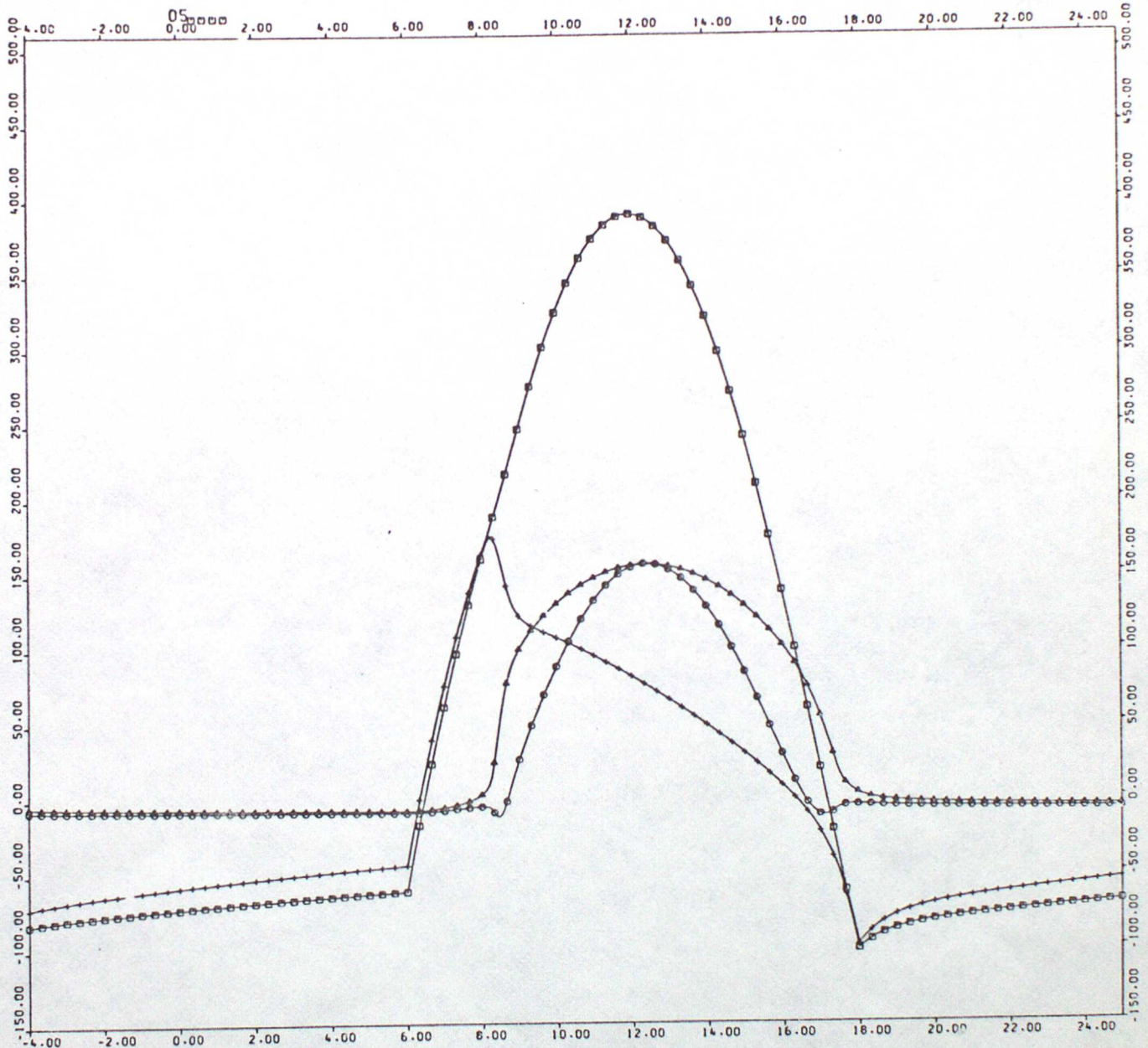


Fig 3 Surface heat fluxes calculated for a clear spring day with $\rho C \sqrt{K} = 950 \text{ MKS}$
 $z_0 = 20 \text{ cm}$, $r_s = 100 \text{ sec m}^{-1}$, $\theta_1 = 285 \text{ K}$, $q_1 = 0.01$, $|u_1| = 2 \text{ m sec}^{-1}$.
 Notice the magnitude and phase of the ground heat flux.

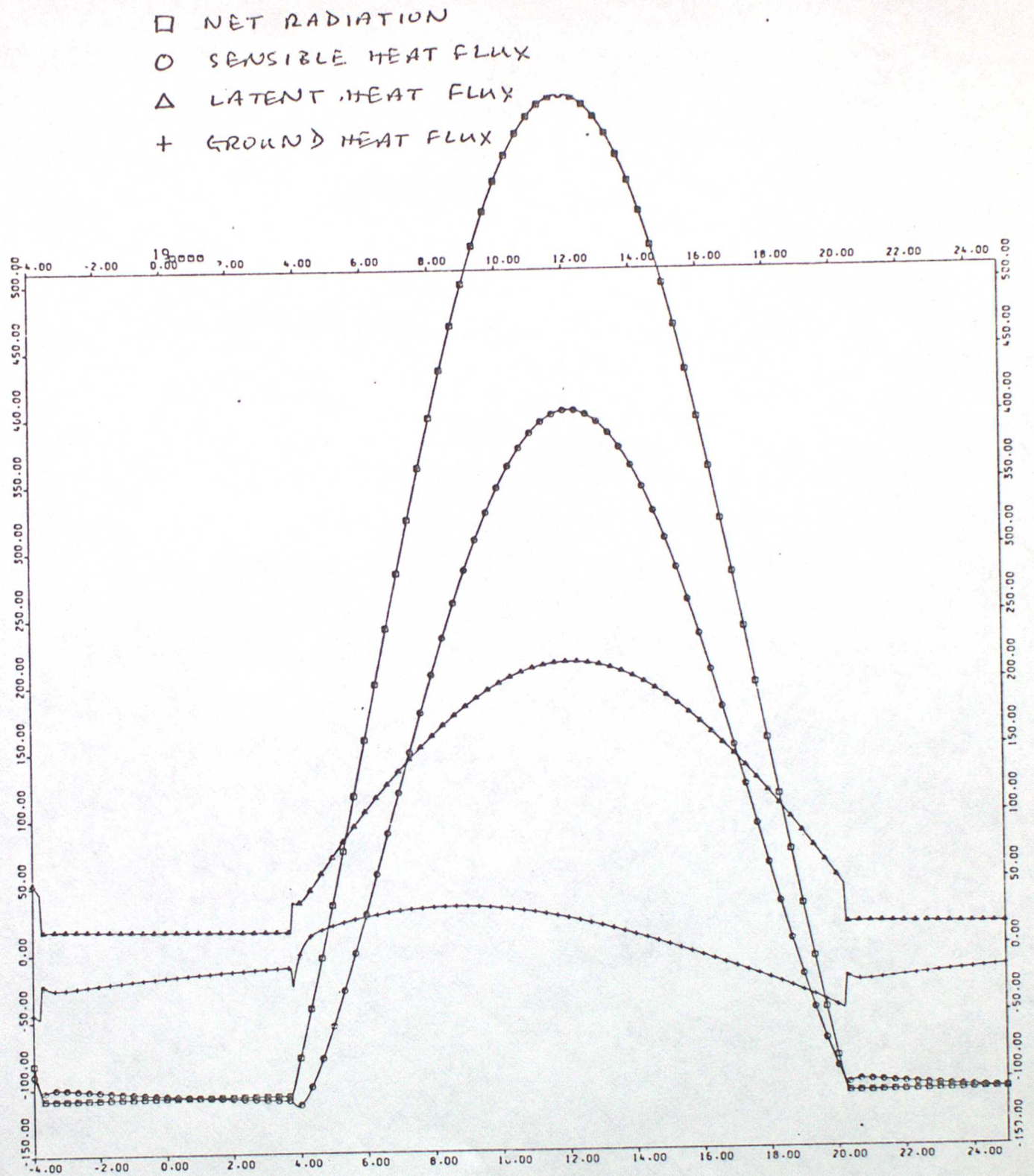


Fig 4 Surface heat fluxes calculated for a clear summer day. $\rho C \sqrt{\pi} = 950 \text{ MKS}$,
 $z_0 = 20 \text{ cm}$, $r_s = 100 \text{ sec m}^{-1}$, $\theta_s = 285 \text{ K}$, $q_1 = 0.01$, $u_1 = 5 \text{ m sec}^{-1}$.
 Notice the discontinuity in the latent heat flux at dawn and dusk.

- NET RADIATION
- SENSIBLE HEAT FLUX
- △ LATENT HEAT FLUX
- + GROUND HEAT FLUX

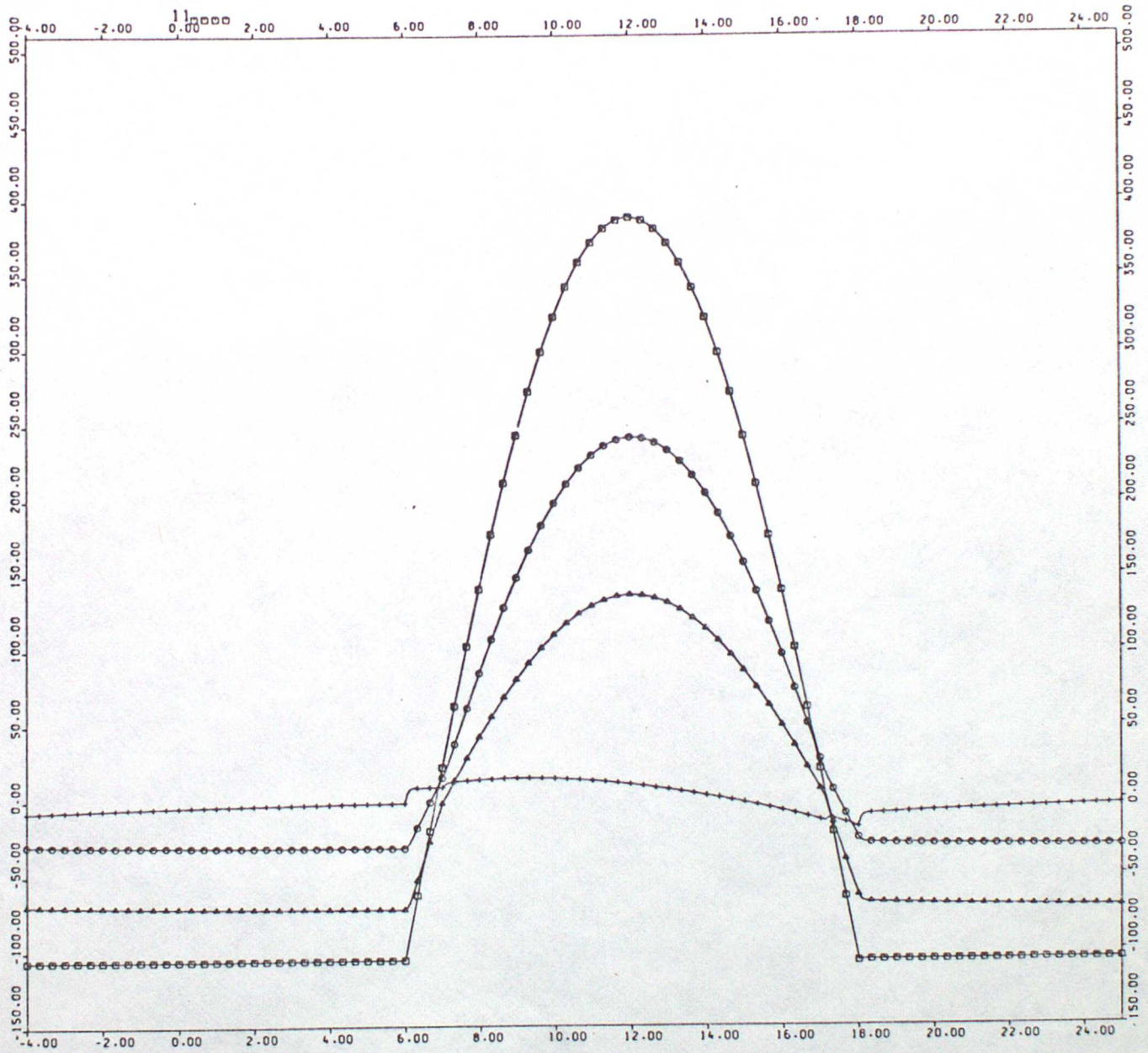


Fig 5 Surface heat fluxes for case A1, which is the control for the comparison shown in Fig 6.

- CONTROL
- z_0 INCREASED 5m \rightarrow 20m
- △ $e_{c,r}$ INCREASED 400 \rightarrow 1400
- + Γ_s INCREASED 50 \rightarrow 100 sec m^{-1}
- x R_i MUTILATED

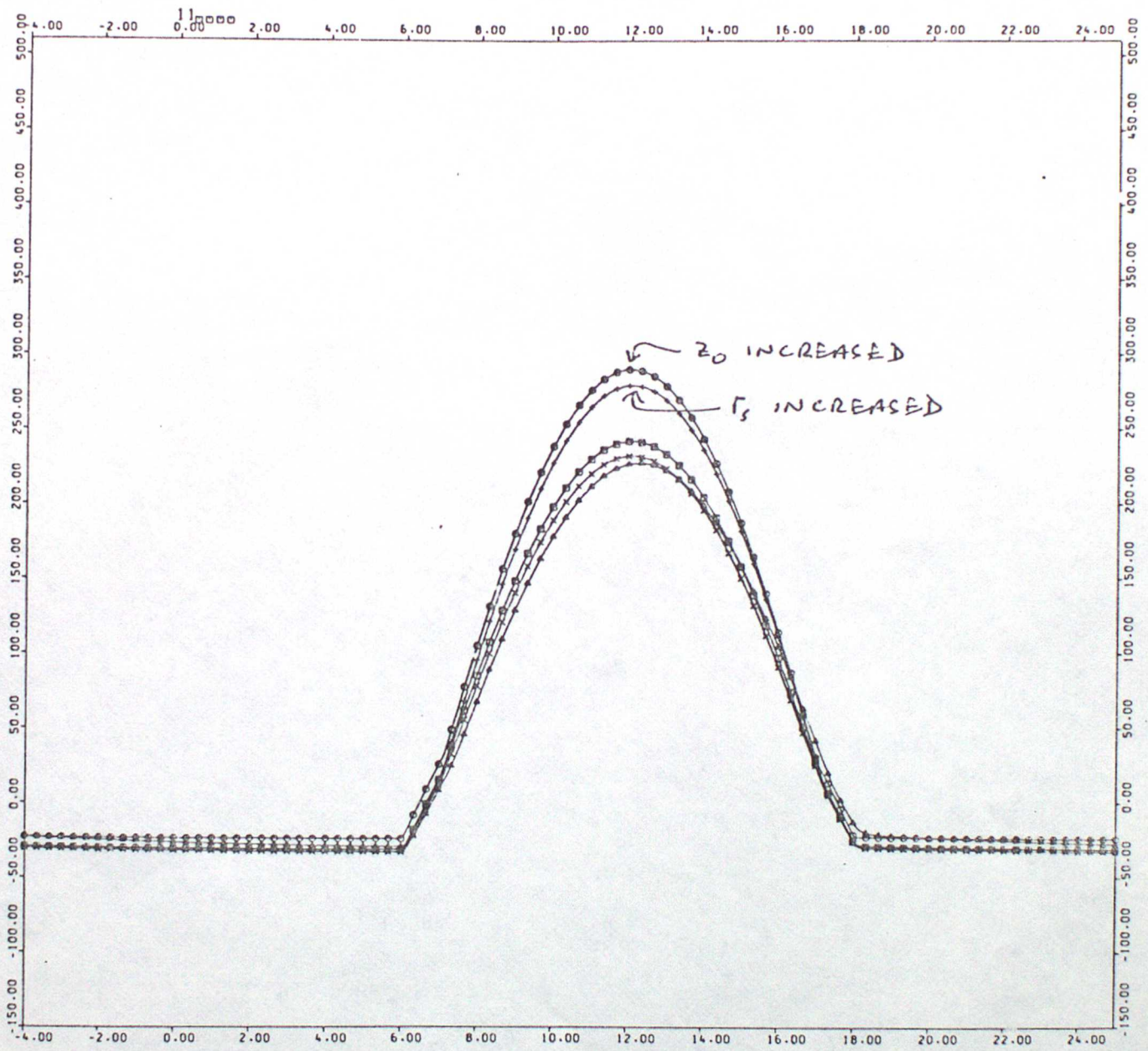


Fig 6 Sensible heat fluxes calculated for 5 different surfaces on a clear spring day with $\theta_i = 280\text{K}$, $q = 0.01$, $1u1 = 5 \text{ m sec}^{-1}$.

- CONTROL
- z_0 INCREASED 5cm \rightarrow 20cm
- △ eC_{JK} INCREASED 400 \rightarrow 1400
- + Γ_s INCREASED 50 \rightarrow 100 cm^{-1}
- x R_i MUTILATED

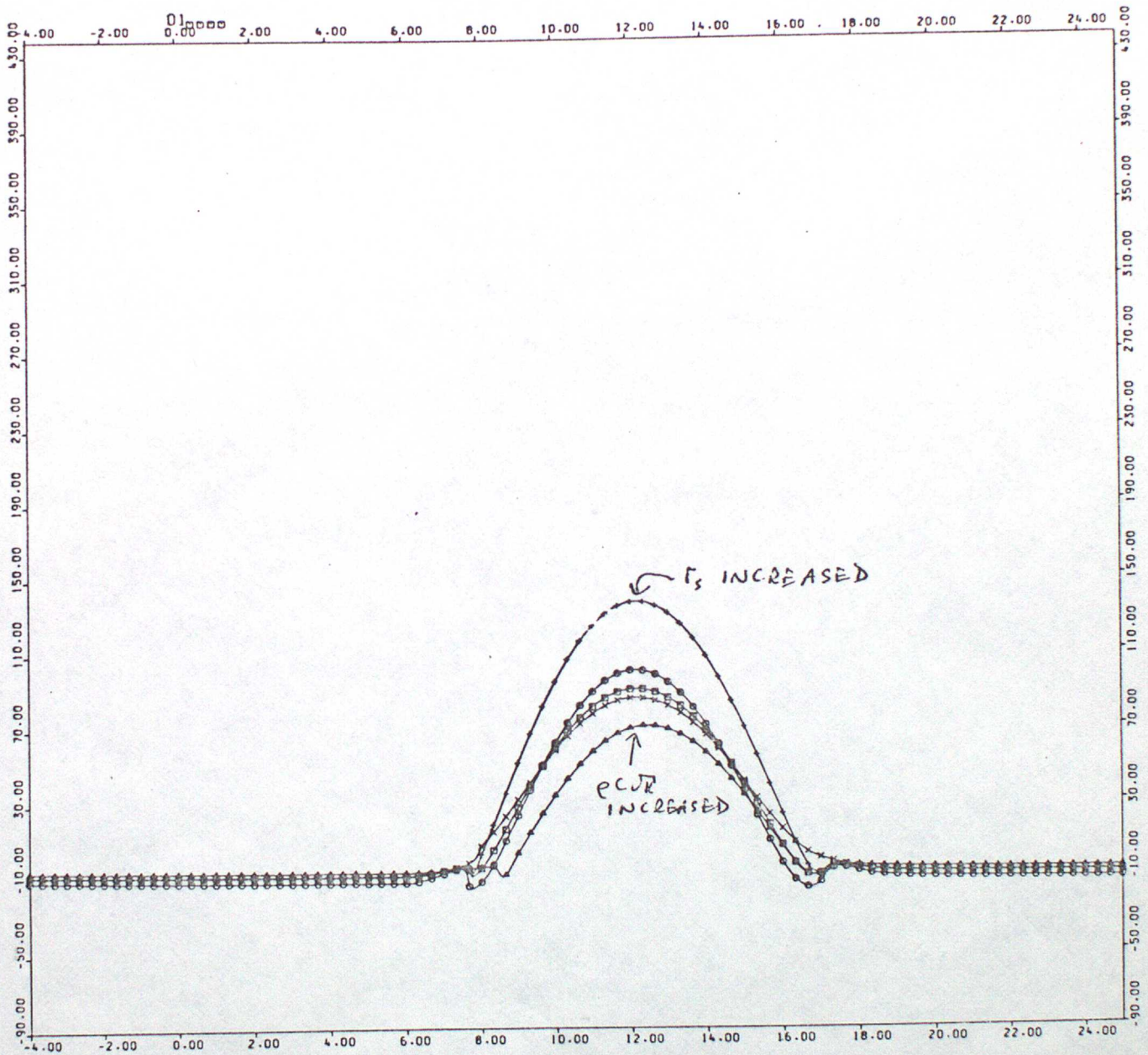


Fig 7 Sensible heat fluxes calculated for 5 different surfaces on a clear spring day with $\theta_s = 290\text{K}$, $q_v = 0.015$, $|\mathbf{u}| = 2 \text{ m sec}^{-1}$.

- NET RADIATION
- SENSIBLE HEAT FLUX
- △ LATENT HEAT FLUX
- + GROUND HEAT FLUX

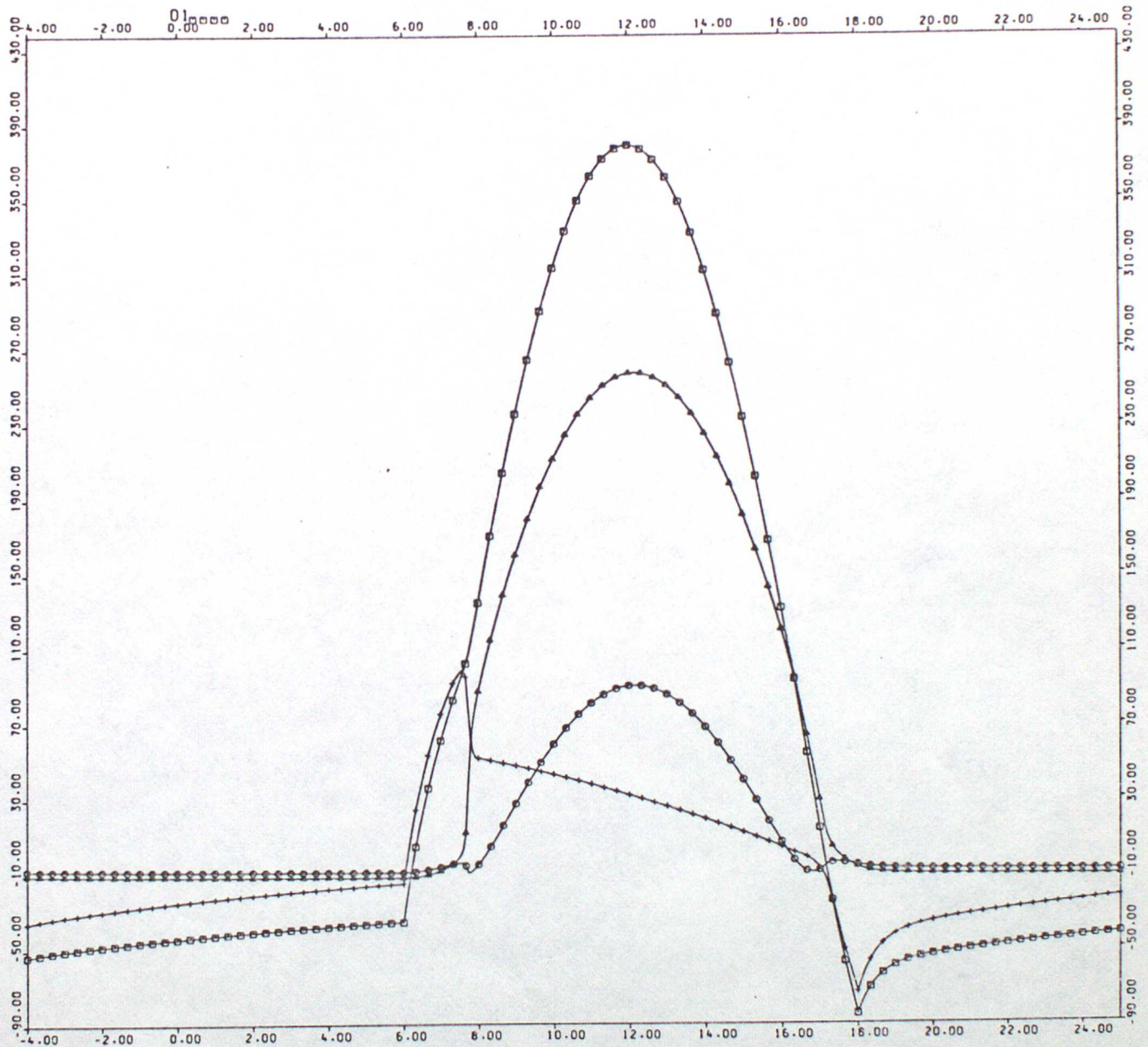


Fig 8 Surface heat fluxes for case B1, which is the control for the comparison shown in Fig 7. $r_s = 50 \text{ sec m}^{-1}$.

- NET RADIATION
- SENSIBLE HEAT FLUX
- △ LATENT HEAT FLUX
- + GROUND HEAT FLUX

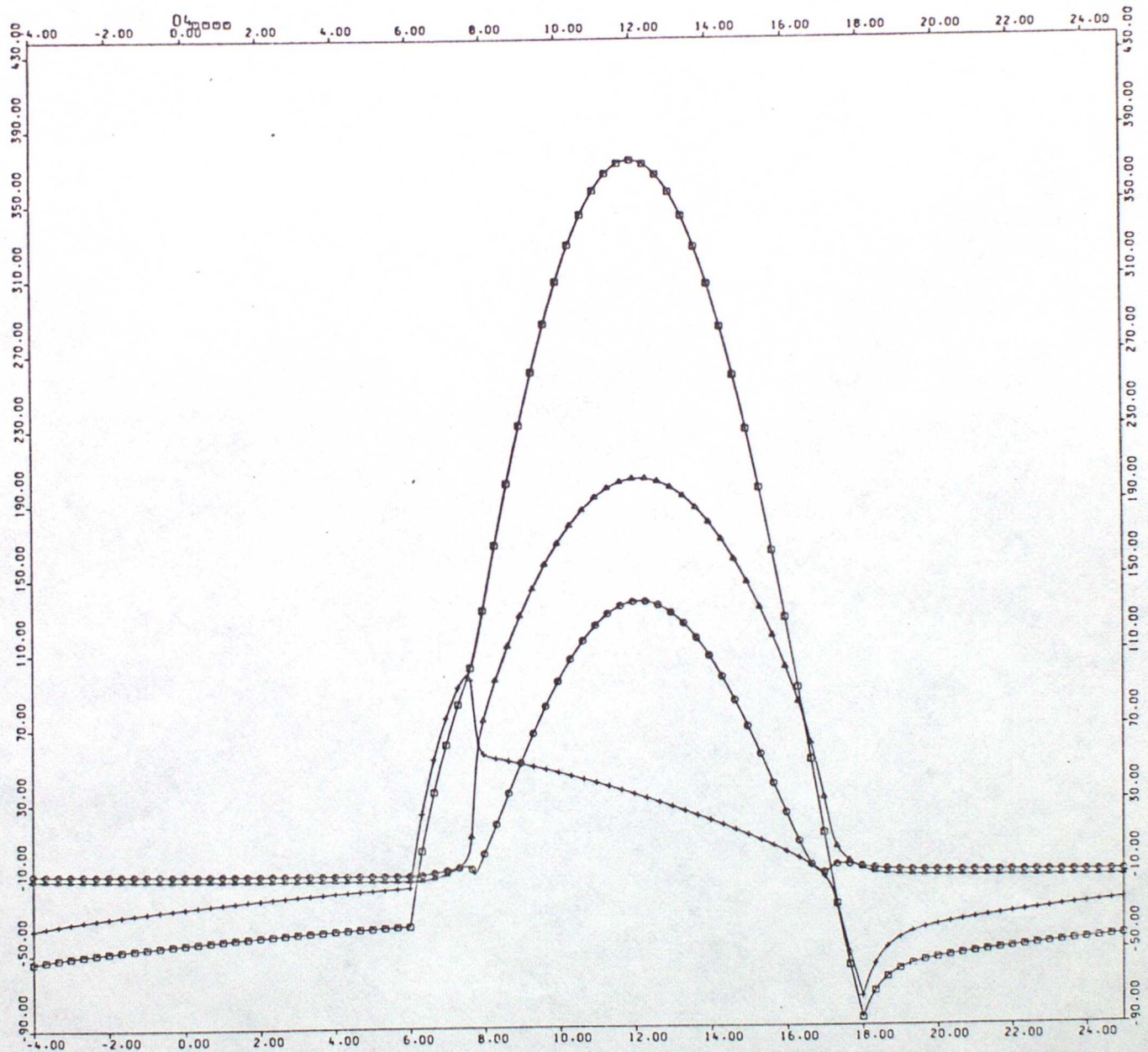


Fig 9 Surface heat fluxes for case B⁴, i.e. the same as B¹ (Fig 7) except for an increase in $r_s = 100 \text{ sec m}^{-1}$.

- NET RADIATION
- SENSIBLE HEAT FLUX
- △ LATENT HEAT FLUX
- + GROUND HEAT FLUX

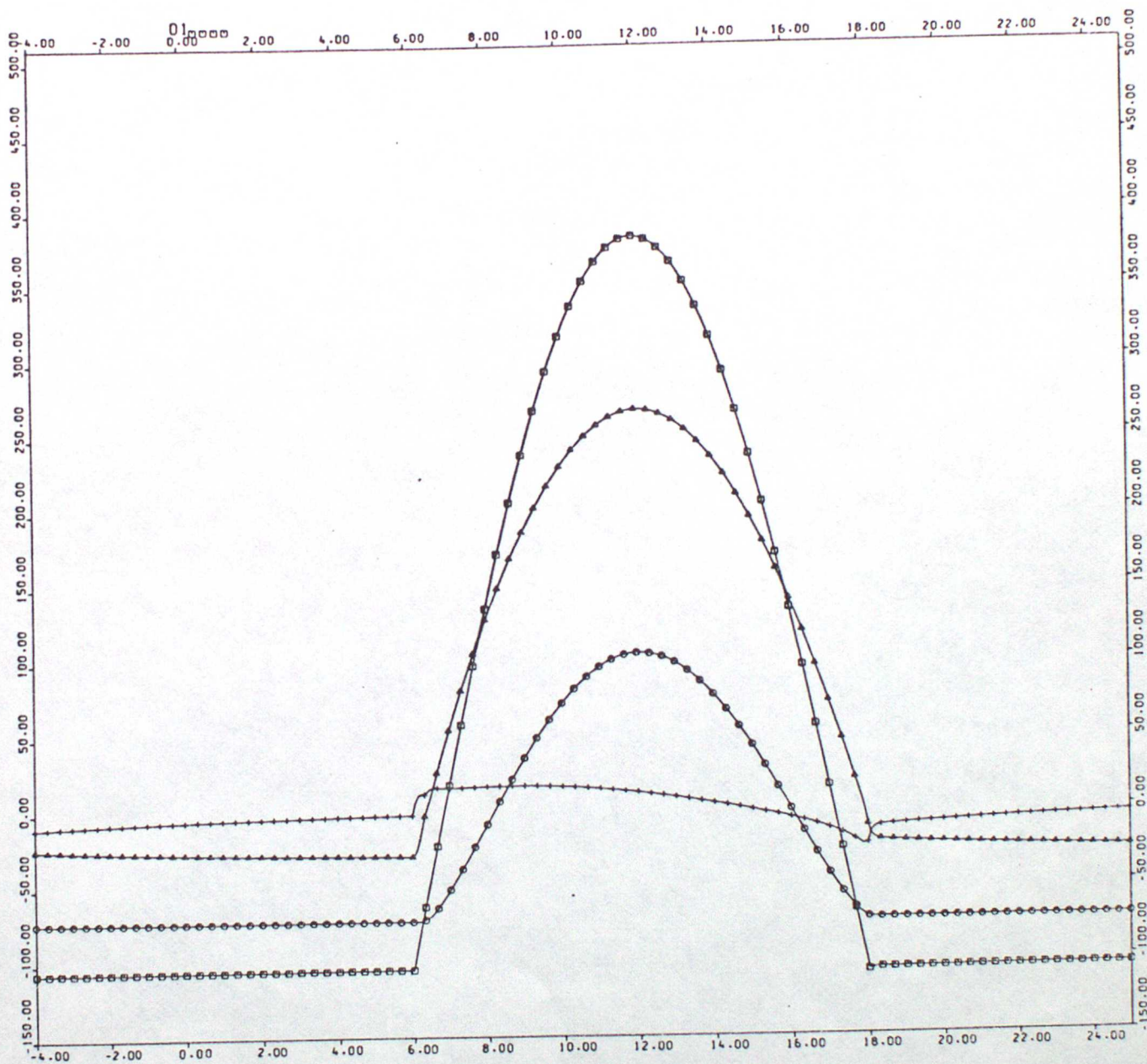


Fig 10 Surface heat fluxes for case D1, which is the control for the comparison shown in Fig 11.

- CONTROL
- z_0 INCREASED 5cm \rightarrow 20cm
- △ $\rho C \sqrt{u}$ INCREASED 400 \rightarrow 1400
- + Γ INCREASED 50 \rightarrow 100 cm^{-1}
- x R_i MUTILATED

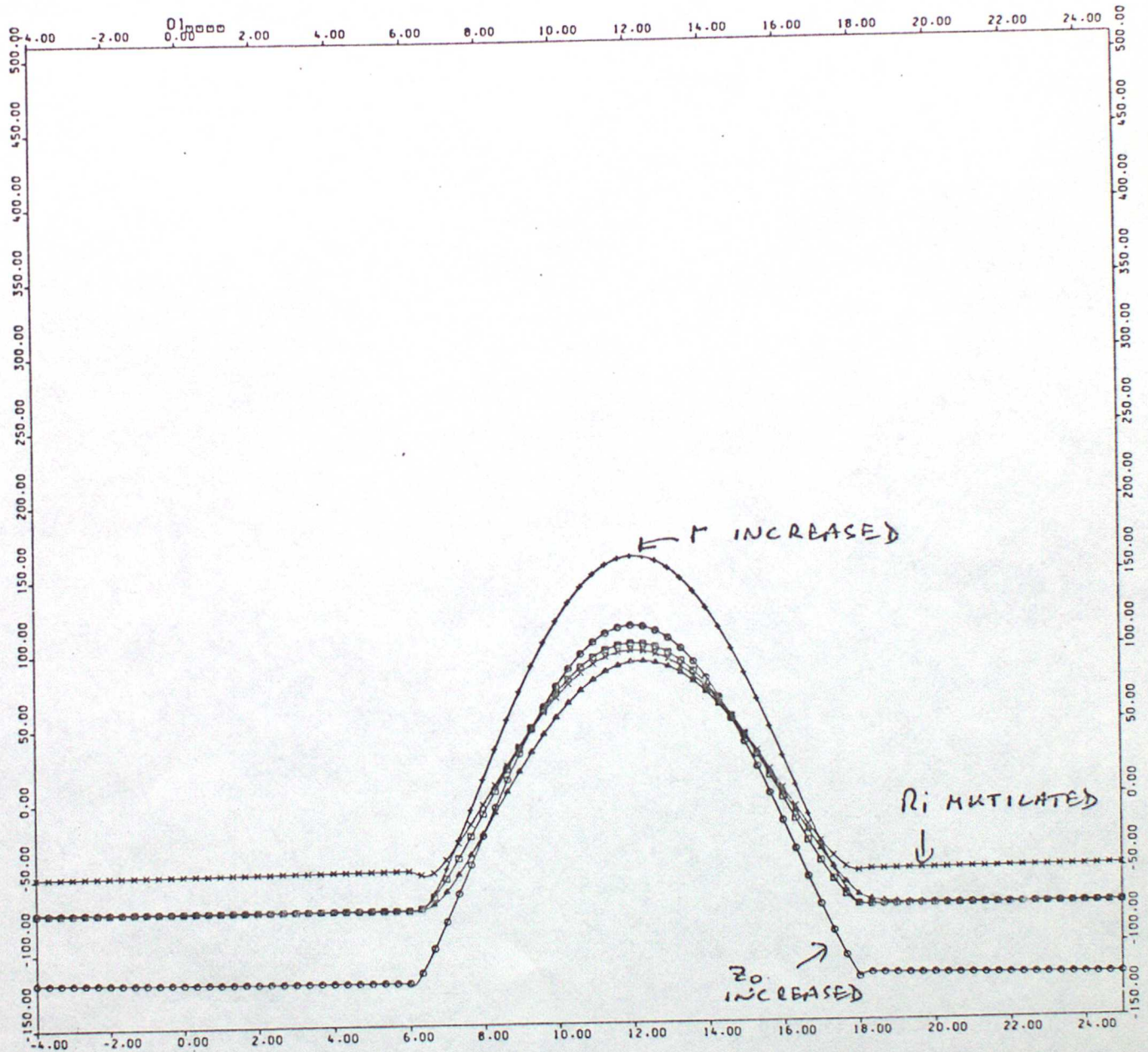
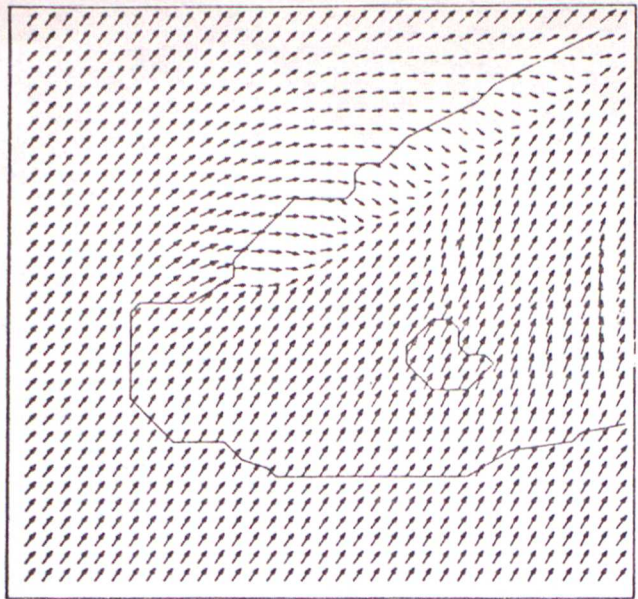
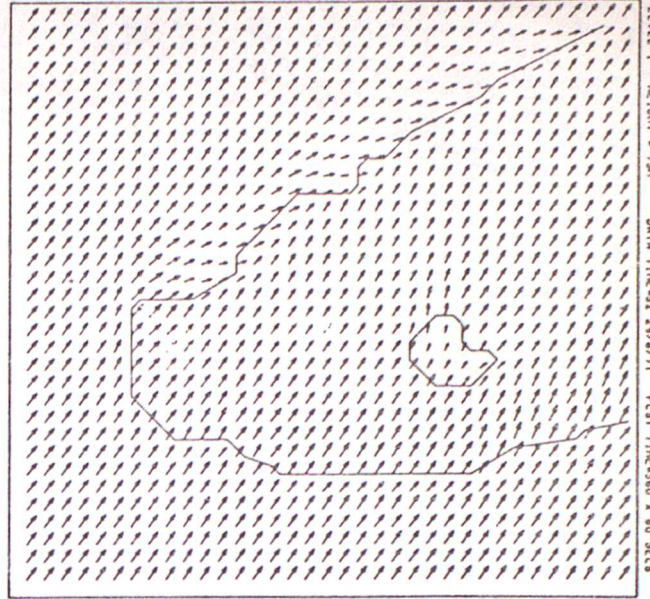


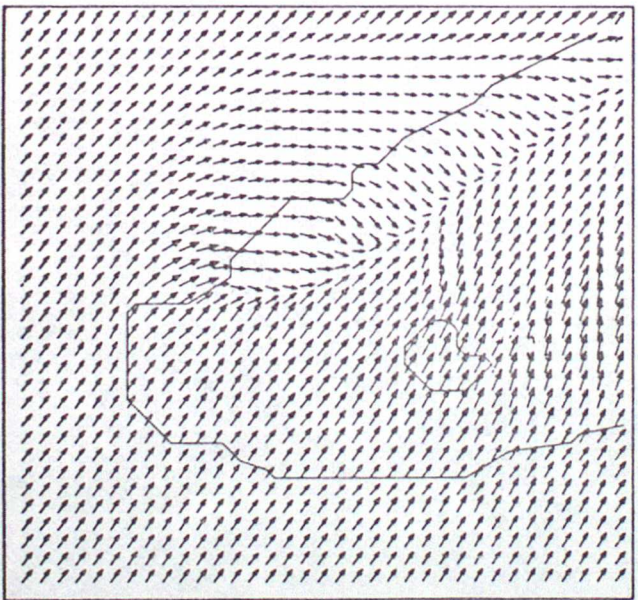
Fig 11 Sensible heat fluxes calculated for 5 different surfaces on a clear spring day with $\theta_i = 290\text{K}$, $q_i = 0.015$; $u_i = 5 \text{ m sec}^{-1}$.



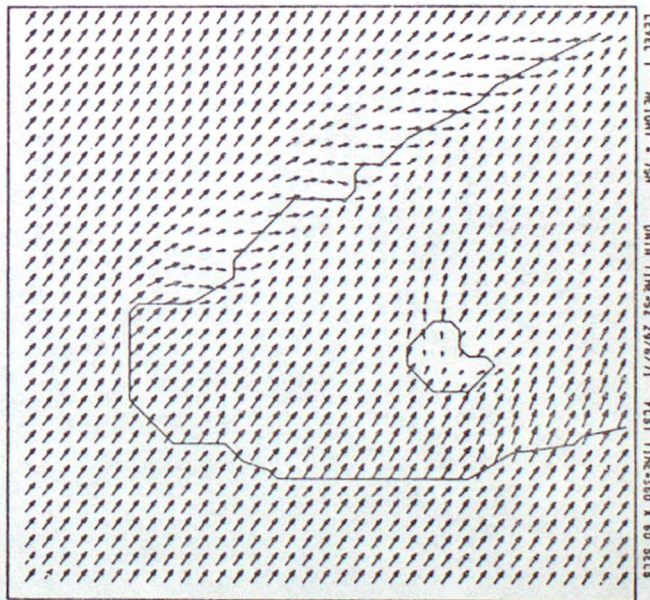
12 HRS



6 HRS



12 HRS



5 HRS

Fig 12 75m winds in two simulations of a Florida sea breeze using different values for r_s (50 sec m^{-1} on the left, 100 sec m^{-1} on the right.)

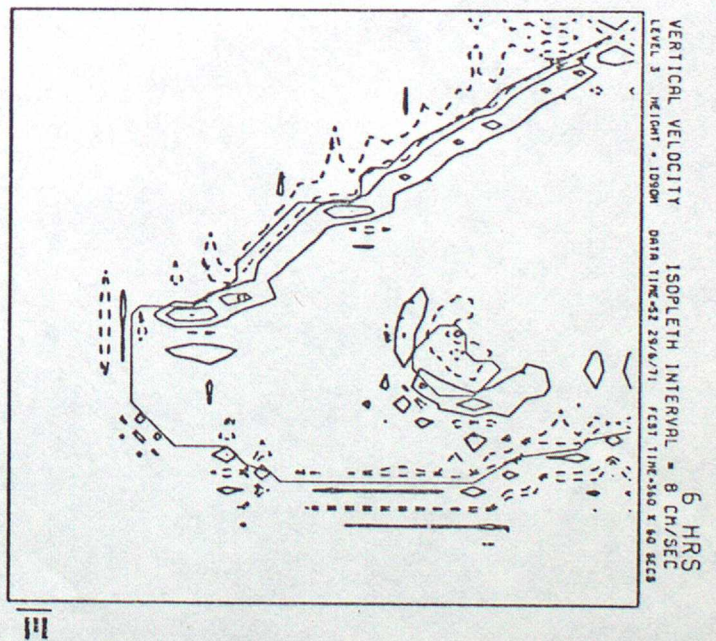
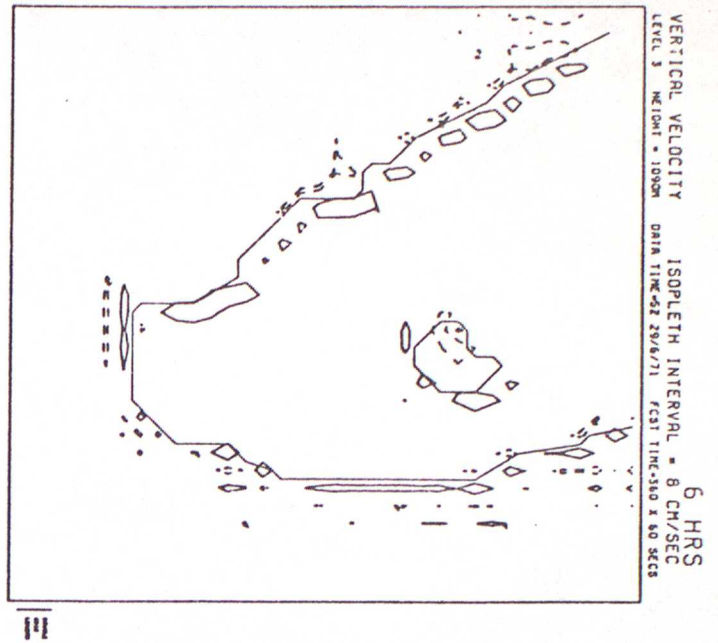


Fig 13 Vertical velocity at 1090m in two simulations of a Florida sea breeze using different values for r_s (50 sec m^{-1} on the left, 100 sec m^{-1} on the right).